Archives of Biochemistry and Biophysics 485 (2009) 109–114

Contents lists available at ScienceDirect

Archives of Biochemistry and Biophysics

journal homepage: www.elsevier.com/locate/yabbi

Molecular interaction between kisspeptin decapeptide analogs and a lipid membrane

Ju Yeon Lee [a], Jung Sun Moon [b], Young-Jae Eu [a], Chul Won Lee [a], Sung-Tae Yang [a], Seung Kyu Lee [a], Hyun Ho Jung [a], Ha Hyung Kim [c], Hyewhon Rhim [d], Jae Young Seong [b], Jae Il Kim [a,e,*]

[a] Department of Life Science, Research Center for Bio-imaging, Gwangju Institute of Science and Technology, Gwangju 500-712, Republic of Korea
[b] Research Laboratory of G Protein Coupled Receptors, Korea University College of Medicine, Seoul 136-705, Republic of Korea
[c] College of Pharmacy, Chung-Ang University, Seoul 156-756, Republic of Korea
[d] Life Sciences Division, Korea Institute of Science and Technology, Seoul 136-791, Republic of Korea
[e] Department of Life Science, Gwangju Institute of Science and Technology, AnyGen Co. Ltd., 1 Oryong-dong, Puk-gu Gwangju 500-712, Republic of Korea

ARTICLE INFO

Article history:
Received 2 January 2009
and in revised form 1 March 2009
Available online 9 March 2009

Keywords:
Kisspeptin
GPR54
Peptide–membrane interaction
NMR
DPC

ABSTRACT

Kisspeptin-10 is the C-terminal decapeptide amide of kisspeptin, an endogenous ligand for GPR54, and exhibits the same binding and agonist activity as the parent molecule. Although GPR54 is a membrane-embedded protein, details of the molecular interaction between kisspeptin-10 and lipid membranes remain unclear. Here, we performed a series of structural analyses using alanine-scanning analogs of kisspeptin-10 in membrane-mimetic medium. We found that there is a close correlation between lipid membrane binding and agonist activity. For instance, the F10A and non-amidated ($NH_2 \rightarrow OH$) analogs showed little or no GPR54-agonist activity and elicited no blue shift in tryptophan fluorescence. NMR analysis of kisspeptin-10 analog in DPC micelles revealed it to contain several tight turn structures, encompassing residues Trp3 to Phe10, but no helical conformation like that seen previously with SDS micelles. Together, our results suggest that kisspeptin-10 may activate GPR54 via a ligand transportation pathway incorporating a lipid membrane.

1. Introduction

G protein-coupled receptors (GPCRs) are the largest family of cell surface membrane receptors and regulate a variety of physiological responses by mediating transmission of extracellular signals into cells [1]. GPR54 is a GPCR family member that is widely expressed in the central nervous system and shares about 45% identity with the galanine receptor [2]. Galanine, however, does not activate or even bind to GPR54. Instead, kisspeptin (also known as metastin), a 54-amino acid peptide fragment of the protein encoded by the *KiSS-1* metastasis suppressor gene, appears to be the cognate ligand for GPR54 [3]. It was previously reported that the 10 C-terminal residues of kisspeptin (kisspeptin-10; Tyr45–Phe54) are critical for specific binding to GPR54 and exhibit agonist activity comparable to that of wild-type kisspeptin [3,4]. Moreover, when the structure–activity relationship of kisspeptin-10 was examined through amino acid substitutions and NMR structure analysis, it was found that the C-terminal region of kisspeptin-10 forms a helical structure in the presence of SDS micelles and plays an especially important role in its binding to and activation of GPR54 [5–7].

On the other hand, although it is well known that GPR54 is a membrane-embedded protein, details of the molecular interaction between kisspeptin-10 and membrane lipids remain unclear. There are two alternative mechanisms by which a ligand may interact with a membrane-embedded receptor [8,9]. The first is a ligand transportation model [10], in which initial binding of a ligand to the membrane is followed by lateral diffusion to the receptor. The second is a direct transfer of the ligand from the aqueous solution to the receptor. In this study, we tried to assess whether the interaction between kisspeptin-10 and GPR54 is consistent with the "membrane compartment theory" [11,12] and the kisspeptin-10 structure in DPC micelles is similar to that in SDS micelles. Interestingly, it was revealed that there is a close correlation between the membrane binding of kisspeptin-10 analogs and their agonist activity.

2. Materials and methods

2.1. Peptide synthesis

All kisspeptin-10 analogs were synthesized through solid phase peptide synthesis performed manually using 9-fluorenylmethoxy-

* Corresponding author. Address: Department of Life Science, Gwangju Institute of Science and Technology, AnyGen Co. Ltd., 1 Oryong-dong, Puk-gu Gwangju 500-712, Republic of Korea. Fax: +82 62 970 2484.
E-mail addresses: jikim@gist.ac.kr, ljy@gist.ac.kr (J.I. Kim).

0003-9861/$ - see front matter © 2009 Elsevier Inc. All rights reserved.
doi:10.1016/j.abb.2009.03.002

carbonyl (Fmoc) chemistry. The peptides were purified using preparative reverse-phase high-performance liquid chromatography (RP-HPLC, Shimadzu, Tokyo, Japan), after which their purity was verified by analytical RP-HPLC. Correct peptide masses were then confirmed by matrix-assisted laser desorption/ionization time-of-flight mass spectrometry (MALDI-TOF MS, Shimadzu, Japan).

2.2. Functional assay of peptide analogs

Rat GPR54 cDNA was amplified by PCR using primers GPR54F (5′-ATCGGAATTCACCATGGCCGCAGAGGCGACGTTG-3′) and rGPR54R (5′-TCACTCGAGTCAGAGTGGGGCAGTGTGTTCATC-3′) from rat brain and inserted at the EcoR I and Xho I sites of pcDNA3. CV-1 cells were maintained in Dulbecco's modified Eagle's medium (DMEM) supplemented with 10% fetal bovine serum. For luciferase assays, cells were plated in 24-well plates 1 day before transfection. They were then transfected with rat GPR54 and c-fos-luc vectors using SuperFect reagent (QIAGEN) according to the manufacturer's instructions. The total amount of DNA used in each transfection was adjusted to 1 μg by adding an appropriate amount of empty pcDNA3. For c-fos promoter-driven luciferase assays, cells were maintained in serum-free DMEM for 16–18 h before treatment with the ligand [13]. They were then harvested 6 h after ligand treatment, and luciferase activity in the cell extracts was determined using a luciferase assay system with a Lumat LB9501 luminometer (EB&G, Berhold, Germany). The values for luciferase activity were then normalized to the activity of the housekeeping enzyme β-galactosidase. Transfection experiments were performed in triplicate and repeated at least three times. All data are presented as means ± SEM.

2.3. Preparation of small unilamellar vesicles

Small unilamellar vesicles (SUVs) were prepared for Trp fluorescence experiments. Phospholipids composed of 1-palmitoyl-2-oleoyl-phosphatidylcholine (POPC)[1] were dissolved in chloroform and dried with a stream of nitrogen to form a thin lipid film. The lipid film was then further dried overnight under a vacuum and resuspended in Tris buffer (10 mM Tris, 0.1 mM EDTA, 150 mM NaCl, pH 7.4) by vortex mixing. Using a titanium-tipped sonicator, the resultant suspension was sonicated under nitrogen in an ice bath for about 20 min until clear. Subsequent dynamic light-scattering experiments confirmed the presence of a main population of vesicles (>96% mass content) with a mean diameter of 42 nm.

2.4. Membrane binding analysis using tryptophan fluorescence

The effect of membrane binding on the fluorescence emission spectrum for the tryptophan residue at N-terminal 3 position of kisspeptin-10 was examined as previously described [14]. Measurements of tryptophan fluorescence were made using a Shimadzu RF 5301 PC spectrofluorometer. POPC liposomes were added to a fixed concentration of peptide (3 μM) dissolved in 3 ml of Tris buffer until the desired peptide/lipid molar (P/L) ratio was reached, after which the tryptophan residue in the peptide was excited at 280 nm (band width, 5 nm), and the emission spectrum was recorded from 300 to 400 nm (band width, 3 nm). Measurements were repeated twice to insure reproducibility.

2.5. Circular dichroism analysis of secondary structure

The circular dichroism (CD) spectra of the peptides were recorded using a Jasco J-710 CD spectrophotometer (Jasco, Tokyo, Japan) with a 1 mm path length cell. Wavelengths were measured from 190 to 250 nm, with 0.1 nm step resolution, 50 nm/min speed, 0.5 s response time, and 1 nm bandwidth. The CD spectra collected for the peptides (150 μM) in the presence of DPC micelles were averaged over 8 scans, and over 4 scans for the peptide in 10 mM sodium phosphate buffer (pH 7.4) at 25 °C. The mean residue ellipticity $[\theta]$ (given in deg cm^2 dmol^{-1}) was calculated as $[\theta] = [\theta]_{obs}$ (MRW/10lc), where $[\theta]_{obs}$ is the ellipticity measured in millidegrees, MRW is the mean residue molecular weight of the peptide, c is the concentration of the sample in mg/mL, and l is the optical path length of the cell in cm. The spectra are expressed as molar ellipticity $[\theta]$ vs. wavelength. The NRMSD (normalized root mean square deviation) indicates the differences between calculated and experimental CD spectra.

2.6. NMR spectroscopy

NMR experiments were carried out at 298 and 313 K in a Bruker DRX 600 spectrometer using test samples containing 1 mM S5A analog dissolved in solution containing 100 mM DPC micelles at pH 3.5. The complete sequence-specific resonance assignments were determined using a standard protocol based on a set of traditional two-dimensional experiments [15]. Processing and analysis of the spectra were done using the XWIN-NMR and ANSIG programs. Cross-peak intensities were quantitatively determined on the basis of the counting levels. For structural calculation, observed NOE data were classified into four distance ranges, 1.8–2.7, 1.8–3.5, 1.8–5.0 and 1.8–6.0 Å, corresponding to strong, medium, weak and very weak NOE values, respectively. Pseudo-atom corrections were used for the methyl protons or the non-stereospecifically assigned methylene protons [16]. The backbone NH–C$^{\alpha}$H coupling constants were estimated from the DQF-COSY spectra and were converted to backbone torsion angle φ constraints based to the following rules. For $^3J_{HN\alpha}$ values of <5.5 Hz, the angle was constrained in the range of $-65 \pm 25°$; for $^3J_{HN\alpha}$ values of >8.0 Hz, it was constrained in the range of $-120 \pm 40°$ [17,18]. All calculations of structure were carried out using the X-PLOR 3.851 program [19]. The three dimensional structures were calculated on the basis of the experimentally derived distance and torsion angle constraints using a dynamically simulated annealing protocol. The calculated structures were analyzed using PROCHECK_NMR [20], PROMOTIF [21] and MOLMOL [22].

3. Results and discussion

3.1. Functionality of kisspeptin-10 analogs

To assess the contribution made by each side-chain of kisspeptin-10 to the molecule's agonist activity toward GPR54 and its interaction with the lipid membrane, we carried out a series of structural analyses, along with functional assay, using a set of alanine-scanning analogs. We initially employed a $G_{q/11}$-linked protein kinase C (PKC)-specific reporter (c-fos-luc) system in a functional assay. As shown in Table 1, analogs with alanine substitutions at Tyr1, Trp3 or Ser5 exhibited activity comparable to wild-type kisspeptin-10, whereas alanine substitutions for residues Asn2, Asn4, Phe6, Gly7, Leu8 or Arg9 caused apparent reductions in agonist activity. In particular, two analogs, F10A and the non-amidated form ($NH_2 \rightarrow OH$), elicited no GPR54 signaling activity. Similarly, it was previously reported that the C-terminal five residues and the amide group of kisspeptin-10 are important for specific binding to GPR54 and potent agonist activity [5,7]. Moreover, Niida et al. demonstrated the importance of the stereochemistry of the C-terminal five residues, using D-amino acid scanning in a pheromone-responsive *lac*Z reporter assay [6]. Although most of

[1] *Abbreviations used:* CD, circular dichroism; POPC, 1-palmitoyl-2-oleoyl-phosphatidylcholine; DPC, dodecylphosphocholine; SDS, sodium dodecyl sulfate.

Table 1
EC_{50} and E_{max} values of kisspeptin-10 and alanine-scanning analogs for rGPR54.

Peptide	EC_{50} (nM)	E_{max}[a]
WT	7.2 ± 1.1	9.30 ± 0.44
Y1A	5.4 ± 2.1	9.60 ± 0.82
N2A	69.2 ± 23.6	10.22 ± 0.99
W3A	1.9 ± 2.2	9.90 ± 1.10
N4A	102.3 ± 58.1	9.29 ± 0.89
S5A	5.2 ± 2.1	9.61 ± 0.76
F6A	204.2 ± 139.9	6.51 ± 0.82
G7A	123.0 ± 32.3	10.57 ± 0.90
L8A	309.0 ± 123.3	3.21 ± 0.37
R9A	134.9 ± 122.8	4.40 ± 0.58
F10A	NR[b]	NR
$NH_2 \rightarrow OH$	NR	NR

[a] Fold induction over basal.
[b] NR, no response for rGPR54.

our results are consistent with earlier reports, it is noteworthy that three analogs, F6A, L8A and R9A, showed comparatively low potency and a partial response that reached only about 50% of the maximum efficacy seen with wild-type kisspeptin-10.

3.2. Membrane binding of kisspeptin-10 analogs

We next analyzed the lipid membrane binding of 8 of the 10 kisspeptin-10 analogs tested by measuring tryptophan fluorescence in the presence and absence of POPC liposomes. Not analyzed were the W3A analog, which has no intrinsic fluorescence, and the R9A analog, which is only poorly fluorescent due to its low solubility. In Tris buffer, the wavelength maxima of the peptides were observed in the range of 350–355 nm, indicating that the tryptophan residue in all the analogs was exposed to the aqueous solvent. It is well known that tryptophan fluorescence undergoes a blue shift when the residue moves from an aqueous to a hydrophobic environment [23]. When POPC liposomes were added to analog-containing buffer to a peptide/lipid (P/L) ratio of 1/100, some of the alanine-scanning kisspeptin-10 analogs showed a significant change in their tryptophan fluorescence spectra (Fig. 1). Most alanine-scanning analogs exhibited blue shifts that were similar to or smaller than that seen with wild-type kisspeptin-10, whereas F6A, F10A and the non-amidated ($NH_2 \rightarrow OH$) form showed little or no blue shift (Fig. 1A). The fluorescence emission spectra for two representative alanine substituted analogs, S5A and F10A, obtained at the indicated P/L ratios are shown in Fig. 1B and C, respectively. Upon addition of POPC liposomes, S5A showed a significant blue shift (about 8 nm), together with an increase in tryptophan fluorescence intensity, indicating movement of the tryptophan residue from the aqueous environment of the buffer to the hydrophobic environment of the liposomes. By contrast, F10A showed no detectable change in its emission maximum, even at P/L ratio of 1/100. It is noteworthy that analog S5A retained GPR54-agonist activity similar to wild-type kisspeptin-10, whereas analog F10A showed no GPR54-agonist activity. This suggests there is a close correlation between the agonist activity of the kisspeptin-10 analogs and their ability to bind to the lipid membrane.

It has been recently reported that the correlation coefficient for a competitive kisspeptin receptor binding and its functional calcium release, with the panel of alanine-scanning analogs, is quite high [7]. In our experimental assay, however, the N4A and S5A analogs had similar blue shift values, but the functional activity of the latter was significantly higher than the former. Similar results were also observed for G7A and N2A analogs. One possible explanation for this discrepancy is that a competitive binding assay by Orsini et al. was performed using kisspeptin-expressing membranes, whereas our binding assay was done by model membrane with POPC liposomes.

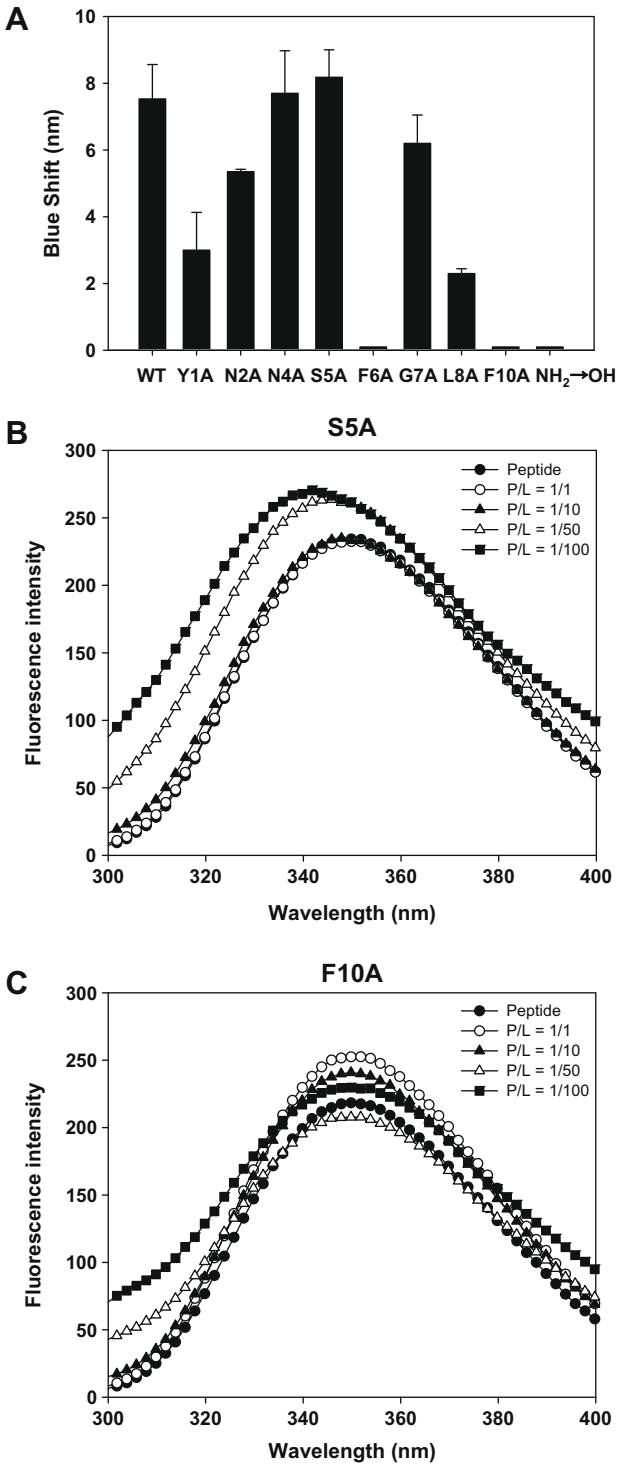

Fig. 1. (A) Fluorescence emission spectra for kisspeptin analogs at a P/L ratio of 1/100 in Tris buffer (pH 7.4) containing 3 μM each peptide at 25 °C. Fluorescence emission spectra for S5A (B) and F10A (C). Spectra were obtained in the presence of POPC liposomes at the indicated P/L ratios in Tris buffer (pH 7.4) containing 3 μM each peptide at 25 °C.

3.3. CD analysis of secondary structure

Wild-type kisspeptin-10 exhibits a poor CD spectrum due to its poor solubility in aqueous solution. We therefore analyzed the CD spectra of two representative analogs, S5A and F10A, in both aqueous buffer and DPC micelles in order to estimate the conforma-

tional change in the peptide backbone induced by binding to a lipid membrane. The CD spectra shown in Fig. 2 were recorded at the indicated peptide/lipid (P/L) ratios and a fixed peptide concentration of 150 μM. Analog S5A showed a primarily unstructured CD pattern with a negative minimum around 198 nm in both aqueous buffer and in the presence of DPC micelles at P/L = 1/10, whereas an ordered structure with a positive maximum near 195 nm and negative double minima near 205 and 215 nm was obtained in the presence of DPC micelles at P/L = 1/100. The DPC-bound conformation of S5A apparently differs from that of a typical α-helix, which has negative double minima at 208 and 222 nm. Interestingly, S5A also exhibited an intermediate CD pattern at P/L = 1/25, indicating the occurrence of a conformational change from a random coil to an ordered structure. Like S5A, analog F10A showed a random coil conformation in both aqueous buffer and in the presence of DPC micelles at P/L = 1/10. Upon increasing the DPC concentration, however, F10A elicited a small red shift (about 3 nm) at its negative minimum, together with weak shoulders around 201 and 218 nm, suggesting only a weak interaction between F10A and DPC micelles. Quantitative CD analysis using CONTINLL [24] revealed that at P/L = 1/100 the structure of S5A can be comprised mainly of β-turn or it can be unordered, while F10A always exhibits an unordered structure (Table 2). Together, these CD results probably indicate that the lipid membrane induces a peptide ligand to assume a more ordered conformation preferable for interaction with the binding site on its receptor.

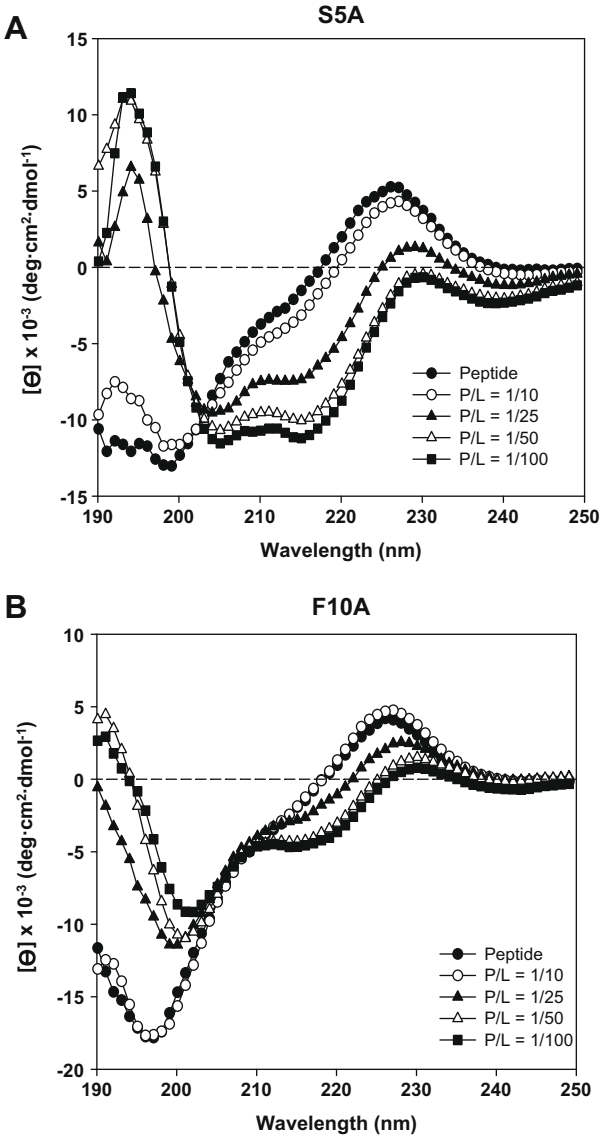

Fig. 2. Circular dichroism spectra for S5A (A) and F10A (B). Spectra were recorded in the presence of DPC micelles at the indicated P/L ratios in 10 mM sodium phosphate buffer (pH 7.2) at 25 °C. Each peptide was used at a concentration of 150 μM.

3.4. NMR structure of membrane-bound S5A analog

To overcome the ambiguity of CD analysis, we carried out an NMR structural analysis of analog S5A. A P/L ratio of 1/100 was used for all NMR experiments. In the presence of DPC micelles, the NOESY spectra showed a small number of short- and medium-range NOEs that were restricted mainly to residues in the C-terminal part of the molecule (Fig. 3A). We detected no secondary structural constraints in the N-terminal part of the molecule (Tyr1–Asn4), reflecting its intrinsic flexibility (Fig. 3B). Notably, NOEs indicating typical of α-helix were not observed. By contrast, cross-peaks characteristic of tight turns, together with coupling constants of more than 8.0 Hz, were observed over the residues extending from Trp3 to Phe10 – i.e., $d_{NN}(i, i+1)$, $d_{\alpha N}(i, i+1)$, $d_{\beta N}(i, i+1)$, and $d_{\alpha N}(i, i+3)$.

To calculate the structures, we used a total of 130 constraints that included 59 distance constraints derived from the interproton NOE cross-peaks, 71 distance constraints derived from the intraproton NOE cross-peaks, and nine dihedral angle constraints derived from the coupling constraints. After carrying out the simulated annealing calculations starting with 100 random structures, we ultimately selected 22 structures with the lowest energy that were in good correspondence with the experimental NMR constraints. The structural statistics for these 22 lowest energy structures evaluated in terms of their structural parameters are summarized in Table 3. The atomic RMSDs about the mean coordinate positions for the residues from Ala5 to Phe10 were 0.54 ± 0.17 Å for the backbone atoms (N, C^{α}, C) and 1.55 ± 0.42 Å for all heavy atoms. In good agreement with the secondary structure predicted from the CD spectra, NMR PROMOTIF analysis for the 22 converged structures revealed that S5A analog contains several tight turn structures, among which the most prevalent were a type I β-turn (residues Trp3–Phe6), two miscellaneous type IV β-turns (residues Asn4–Gly7 and Gly7–Phe10), and a γ-turn (Ala5–Gly7) (Fig. 4A). It is interesting that the C-terminal part of kisspeptin-10 forms a hydrophobic cluster, consisting of two aromatic residues (Phe6 and Phe10) and one aliphatic side-chain (from Leu8), which might facilitate interaction with the hydrophobic carbon chains of the lipid membrane (Fig. 4B).

A recent NMR study showed that, in the presence of SDS micelles, a down-sized kisspeptin assumes a relatively stable helical

Table 2
Secondary structure analysis of S5A and F10A (peptide/lipid = 1/100) using CONTINLL software.

	α-Helix(r)	α-Helix(d)	β-Strand(r)	β-Strand(d)	β-Turn	Unordered	NRMSD
S5A	0.000	0.085	0.130	0.135	0.316	0.335	0.102
F10A	0.000	0.031	0.200	0.124	0.200	0.445	0.082

α-Helix(r), regular α-Helix; α-Helix(d), distorted α-Helix; β-Strand(r), regular β-Strand; β-Strand(d), distorted β-Strand.

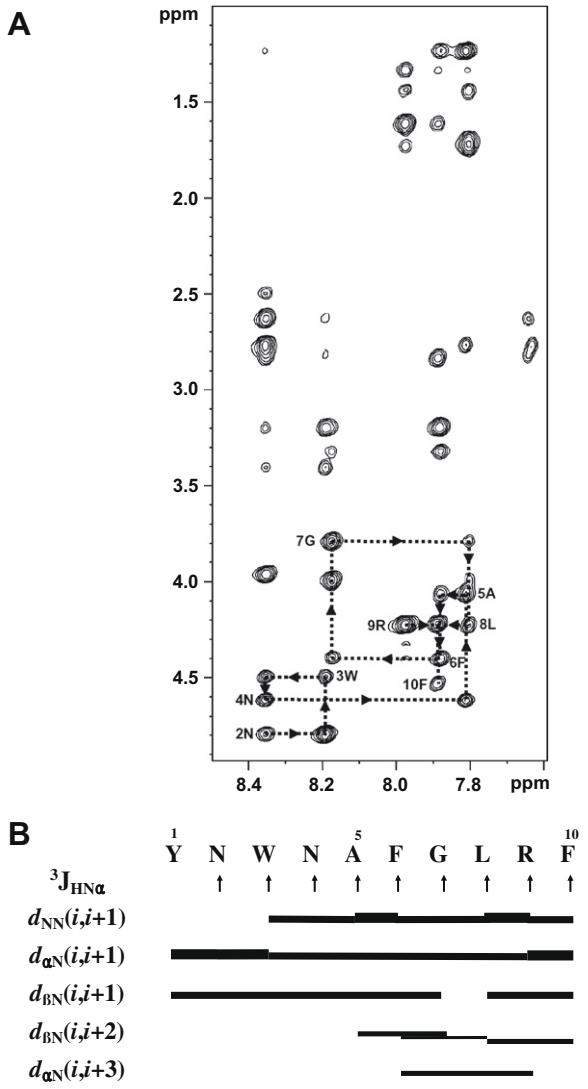

Fig. 3. (A) Partial 600 MHz NOESY spectrum for 1 mM S5A in presence of membrane-mimetic solvent (100 mM DPC), recorded at 298 K with a mixing time of 150 ms. The αN finger print region is presented with sequential $d_{\alpha N}(i, i+1)$ connectivities using single-letter amino acid abbreviations. (B) Summary of the inter-residue NOE connectivities and $^3J_{HN\alpha}$ coupling constants observed in S5A. The NOEs were classified as strong, medium, weak or very weak, which is indicated by the height of the filled bars. The values of the $^3J_{HN\alpha}$ coupling constants are indicated by the ↑ (>8 Hz) and ↓ (<5.5 Hz) symbols.

conformation from Asn4 to Phe10, which encompasses several functionally important residues [7]. In contrast, in the presence of DPC micelles, which mimic the mammalian membrane, our NMR solution structure revealed the occurrence of several tight turn structures, encompassing residues Trp3 to Phe10, but not a helical conformation. One possible explanation for this discrepancy is the difference in the lipid membrane used for the NMR experiments, as SDS micelles have a negatively charged surface, while DPC micelles have a neutral zwitterionic surface. Several structural studies with the lipid membrane indicated that membrane environment induces stable secondary structure in flexible peptide ligands and membrane-induced peptide structures could be correlated with their bioactivity [11,12].

In summary, our finding that there is a close correlation between the membrane binding of kisspeptin-10 analogs and their agonist activity implies that endogenous kisspeptin may activate GPR54 via a ligand transportation pathway, incorporating a lipid membrane, but not a direct interaction with a receptor.

Table 3
Structural statistics for converged 22 structures of S5A bound to DPC micelles.

RMS deviations from experimental distance constraints (Å)[a]	0.0400 ± 0.0022
RMS deviations from experimental distance constraints (deg.)[a]	0.3883 ± 0.1746
Energetic statictics (kcal mol^{-1})[b]	
F_{NOE}	0.0986 ± 0.0905
F_{tor}	1.5001 ± 0.0954
F_{repel}	10.1122 ± 1.1600
E_{L-J}	−24.0856 ± 6.2888
RMS deviations from idealized geometry	
Bonds (Å)	0.0032 ± 0.0002
Angles (deg.)	0.4747 ± 0.0203
Impropers (deg.)	0.2864 ± 0.0092
X-PLOR potential energy (E_{total})	25.1118 ± 2.1827
Ramachandran analysis (%) (residues 5–10)[c]	
Most favored regions	27.3%
Additionally allowed regions	72.7%
Generously allowed regions	0%
Disallowed regions	0%

None of these 22 structures exhibited distance violation >0.3 Å or dihedral angle violations >3°.

[a] The number of each experimental constraint used in the calculations is given in parentheses.

[b] F_{NOE}, F_{tor}, and F_{repel} are the energies related to the NOE violations, the torsion angle violations and the van der Waals repulsion term, respectively. The values of the force constants used for these terms are the standard values as depicted in the X-PLOR 3.851 manual (20). E_{L-J} is the Lennard–Jones van der Waals energy calculated with the CHARMm empirical energy function. E_{L-J} was not used in the dynamical simulated annealing calculations.

[c] The program PROCHECK_NMR [21] was used to assess the stereochemical quality of the structures.

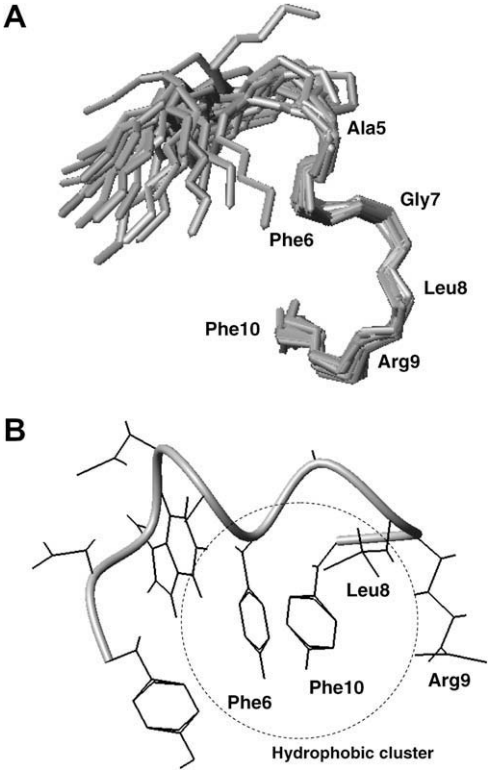

Fig. 4. (A) The best-fit superposition of the backbone atoms (N, C^{α}, and C) as ribbon tubes for the 22 converged structures of S5A in the presence of DPC micelles. Fitting was for the C-terminal residues (positions 5–10), which are designated by the amino acid three-letter codes. (B) Model of the structure having the lowest energy value among the 22 converged structures showing the orientation of side-chains. The important C-terminal residues are marked as the hydrophobic cluster.

Acknowledgment

This study was totally supported by the Brain Research Center of the 21st Century Frontier Research Program (M103KV010006-06K2201-00610).

References

[1] M.C. Lagerström, H.B. Schiöth, Nat. Rev. Drug Discov. 7 (2008) 339–357.
[2] D.K. Lee, T. Nguyen, G.P. O'Neill, R. Cheng, Y. Liu, A.D. Howard, N. Coulombe, C.P. Tan, A.T. Tang-Nguyen, S.R. George, B.F. O'Dowd, FEBS Lett. 446 (1999) 103–107.
[3] M. Kotani, M. Detheux, A. Vandenbogaerde, D. Communi, J.M. Vanderwinden, E. Le Poul, S. Brézillon, R. Tyldesley, N. Suarez-Huerta, F. Vandeput, C. Blanpain, S.N. Schiffmann, G. Vassart, M. Parmentier, J. Biol. Chem. 276 (2001) 34631–34636.
[4] T. Ohtaki, Y. Shintani, S. Honda, H. Matsumoto, A. Hori, K. Kanehashi, Y. Terao, S. Kumano, Y. Takatsu, Y. Masuda, Y. Ishibashi, T. Watanabe, M. Asada, T. Yamada, M. Suenaga, C. Kitada, S. Usuki, T. Kurokawa, H. Onda, O. Nishimura, M. Fujino, Nature 411 (2001) 613–617.
[5] K. Tomita, A. Niida, S. Oishi, H. Ohno, J. Cluzeau, J.M. Navenot, Z.X. Wang, S.C. Peiper, N. Fujii, Bioorg. Med. Chem. 14 (2006) 7595–7603.
[6] A. Niida, Z. Wang, K. Tomita, S. Oishi, H. Tamamura, A. Otaka, J.M. Navenot, J.R. Broach, S.C. Peiper, N. Fujii, Bioorg. Med. Chem. Lett. 16 (2006) 134–137.
[7] M.J. Orsini, M.A. Klein, M.P. Beavers, P.J. Connolly, S.A. Middleton, K.H. Mayo, J. Med. Chem. 50 (2007) 462–471.
[8] R. Bader, O. Zerbe, Chembiochem 6 (2005) 1520–1534.
[9] R. Sankararamakrishnan, Biosci. Rep. 26 (2006) 131–158.
[10] H. Inooka, T. Ohtaki, O. Kitahara, T. Ikegami, S. Endo, C. Kitada, K. Ogi, H. Onda, M. Fujino, M. Shirakawa, Nat. Struct. Biol. 8 (2001) 161–165.
[11] R. Schwyzer, Biopolymers 31 (1991) 785–792.
[12] R. Schwyzer, Biopolymers 37 (1995) 5–16.
[13] D.Y. Oh, L. Wang, R.S. Ahn, J.Y. Park, J.Y. Seong, H.B. Kwon, Mol. Cell. Endocrinol. 205 (2003) 89–98.
[14] S.T. Yang, J.Y. Lee, H.J. Kim, Y.J. Eu, S.Y. Shin, K.S. Hahm, J.I. Kim, FEBS J. 273 (2006) 4040–40454.
[15] K. Wuthrich, NMR of Protein and Nucleic Acids, John Wiley and Sons, New York, 1986.
[16] K. Wüthrich, M. Billeter, W. Braun, J. Mol. Biol. 169 (1983) 949–961.
[17] A. Pardi, M. Billeter, K. Wüthrich, J. Mol. Biol. 180 (1984) 741–751.
[18] A.D. Kline, W. Braun, K. Wüthrich, J. Mol. Biol. 204 (1988) 675–724.
[19] A.T. Brunger, X-PLOR Manual, Version 3.1, Yale University, New Haven, CT, 1993.
[20] R.A. Laskowski, J.A. Rullmannn, M.W. MacArthur, R. Kaptein, J.M. Thornton, J. Biomol. NMR 8 (1996) 477–486.
[21] E.G. Hutchinson, J.M. Thornton, Protein Sci. 5 (1996) 212–220.
[22] R. Koradi, M. Billeter, K. Wüthrich, J. Mol. Graph. 14 (1996) 29–32.
[23] J.R. Lakoxicz, Principles of Fluorescence Spectroscopy, 2nd ed., Kluwer Academic/Plenum, New York, 1999.
[24] N. Sreerama, R.W. Woody, Anal. Biochem. 287 (2000) 252–260.